CEBAF PROPOSAL COVER SHEET

This Proposal must be mailed to:

CEBAF
Scientific Director's Office
12000 Jefferson Avenue
Newport News, VA 23606

and received on or before OCTOBER 31, 1989

A. TITLE: Electroproduction of Baryon Resionances at High Q^2

B. CONTACT PERSON: Paul Stoler

ADDRESS, PHONE AND BITNET:

RPI - Phys. Dept., Troy, NY
518/276-8333 STOLER@RPITSMTS

C. THIS PROPOSAL IS BASED ON A PREVIOUSLY SUBMITTED LETTER OF INTENT

/X/ YES
/ / NO

IF YES, TITLE OF PREVIOUSLY SUBMITTED LETTER OF INTENT

Electromagnetic Properties of Baryon Resonances at High Momentum Transfer

D. ATTACH A SEPARATE PAGE LISTING ALL COLLABORATION MEMBERS AND THEIR INSTITUTIONS

==========

(CEBAF USE ONLY)

Proposal Received 10-31-89

Log Number Assigned PR-89-040

By IKES
contact: Stoler

Study of Electromagnetic Excitation of Baryon Resonances with the CEBAF Large Acceptance Spectrometer

The N* Collaboration

V. Burkert, D. Joyce, B. Mecking, M.D. Mestayer, B. Niczyporuk, E.S. Smith, A. Yegneswaran
CEBAF, Newport News, Virginia

R. Minehart, D. Day, J. McCarthy, O. Rondon-Aramayo, R. Sealock, S. Thornton, H.J. Weber
University of Virginia, Charlottesville, Virginia

P. Stoler, G. Adams, L. Ghedira, N. Mukhopadyay
Rensselaer Polytechnic Institute, Troy, New York

R. Arndt, D. Jenkins, D. Roper
Virginia Polytechnic Institute and State University, Blacksburg, Virginia

D. Isenhower, M. Sadler
Abilene Christian University, Abilene, Texas

D. Keane, M. Manley
Kent State University, Kent, Ohio

S. Dytman, T. Donoghue
University of Pittsburg, Pittsburg, Pennsylvania

C. Carlson, H. Funsten
College of William and Mary, Williamsburg, Virginia

D. Doughty
Christopher Newport College, Newport News, Virginia

L. Dennis, K. Kemper
Florida State University, Tallahassee, Florida

K. Giovanetti
James Madison University, Harrisonburg, Virginia

J. Lieb
George Mason University, Fairfax, Virginia

W. Kim
University of New Hampshire, Durham, New Hampshire

C. Stronach
Virginia State University, Petersburg, Virginia

M. Gai
Yale University, New Haven, Connecticut

Proposal 4

Proposal to the
CEBAF
Program Advisory Committee

The Study of Excited Baryons at High Momentum Transfer with the CLAS

The N* Group

-in the CLAS Collaboration-

G. Adams, R. Arndt, V. Burkert, C. Carlson, D. Day, L. Dennis, T. Donaghue, D. Doughty, S. Dytman, H. Funsten, M. Gai, L. Ghedira, K. Giovanetti, D. Isenhower, D. Jenkins, D. Joyce, D. Keane, K. Kemper, W. Kim, M. Manley, J. McCarthy, B.Mecking, M.D. Mestayer, R. Minehart, N. Mukhopadyay, B. Niczyporuk, O. Rondon-Aramayo, D. Roper, M. Sadler, R. Sealock, E.S. Smith, P. Stoler, C. Stronach, S. Thornton, H.J. Weber, A. Yegneswaran

P. Stoler and V. Burkert
Spokespersons

Abstract: It is proposed to measure the properties of excited nucleons at high Q^2 by means of exclusive single meson production. The motivation is to investigate short range phenomena in the transition from the non-perturbative QCD regime, where theoretical descriptions have used non-relativistic, and relativized mean field models, to those involving perturbative QCD (pQCD). Initial measurements will be caried out at $Q^2 \sim$ 3 - 4 GeV^2/c^2 at an incident electron energy of 4 GeV, utilizing the initial detection capabilities of the CLAS spectrometer. Later measurements will be extended to higher Q^2 as electron detection acceptance and/or the electron beam energy increases. Among the specific issues we wish to investigate are whether the form-factors of the larger amplitude transitions approach the Q^2 dependence predicted by pQCD calculations, whether there is significant longitudinal strength in the region of the Roper resonance, and whether the anomalous behavior of the $S_{11}(1535)$ form factor continues at high Q^2.

Resonance Studies at High Q^2

I. Introduction

It is proposed to measure exclusive single meson production on nucleons in the resonance region (W = 1.2 to 1.8 GeV) at high Q^2 ($Q^2 \gtrsim 3$ GeV^2/c^2). This will permit the examination of short range phenomena in a kinematic region which has never before been studied by exclusive reactions. Even the available exclusive data is sparse, and would be greatly improved as a result of these measurements. The motivation is to study the transition from the non-perturbative QCD regime (npQCD), where theoretical descriptions have used non-relativistic, and relativized mean field models, to those involving perturbative QCD (pQCD). In this proposal, there are several specific issues we will address involving the high Q^2 behavior of the transition form factors for resonances such as, the $P_{33}(1232)$, $P_{11}(1440)$, $D_{13}(1530)$, $S_{11}(1535)$, and $F_{15}(1688)$.

This is a long range program which will incrementally utilize the maximum CEBAF electron beam energy, and the maximum acceptance and luminosity capabilities of the CLAS spectrometer. The initial measurements will utilize an incident electron energy of 4 GeV, and the initial complement of CLAS detectors. This will enable us to investigate phenomena in the range of Q^2 from 3 to 4 GeV^2/c^2. As the available acceptance and energy increase, studies will be extended to higher Q^2. Due to the small cross sections, kinematic intervals in Q^2 and W will be greater than for the other experiments in the N* program; in particular, typical intervals of $\Delta Q^2 = 1$ GeV^2/c^2 and $\Delta W = 50$ MeV are considered here.

II. Physics Motivation

(The definitions and relationships between the Electromagnetic helicity amplitudes, the Walker helicity elements, and the CGLN multipoles which are used in the text may be found in the Appendix)

Transition from npQCD to pQCD

The Q^2 regime from 3 to 6 GeV^2/c^2 covers the transition region from the low Q^2, or npQCD regime, to the higher Q^2 or asymptotic freedom regime, where pQCD techniques are appropriate.

Using helicity conservation, which is expected to be valid in the limit of free massless spin 1/2 particles, the $A_{1/2}$ amplitudes should dominate with increasing Q^2 (cf Ca-89). This turnover is also predicted by quark potential models. Published exclusive data (Fo-83) up to 1 GeV^2/c^2, as well as unpublished data (Ha-79) at at $Q^2 > 1$ GeV^2/c^2 suggest that for the D_{13} and F_{15} states,the crossover from $A_{3/2}$ to $A_{1/2}$ dominance may occur for Q^2 as low as 1 fm^{-1} or less.

The analogous situation for the delta is not as clear, since $A_{1/2}$ dominance implies that $M_{1+} = E_{1+}$, whereas experimentally one finds that $E_{1+} \ll M_{1+}$, even in the Q^2 region where the crossover appears to occur for the D_{13} and F_{15} states. However, it is pointed out in Ca-89 that existing data may also be compatible with $E_{1+}(E2) \sim M_{1+}(M1)$ if the assumption in the analysis of M_{1+} dominance is relaxed. Clearly, high quality data is needed here.

pQCD calculations using constituent quark Feynman diagrams, such as indicated in Figure 1, also make simple predictions about the Q^2 dependence of the helicity amplitudes: in particular $Q^3A_{1/2} \rightarrow$ const., and $Q^5A_{3/2} \rightarrow$ const. These are obtained by

assuming a quark-gluon vertex followed by successive single gluon propagators connecting the remaining two quarks. At this time published $A_{1/2}$ data exists for the S_{11} state at $Q^2 < 3$ GeV^2/c^2, and for the D_{13} and F_{15} at $Q^2 < 1\ GeV^2/c^2$, with unpublished results extending the measurements to 3 GeV^2/c^2 The existing data is shown in Figure 2, where no leveling off to the predicted scaling rules is observed.

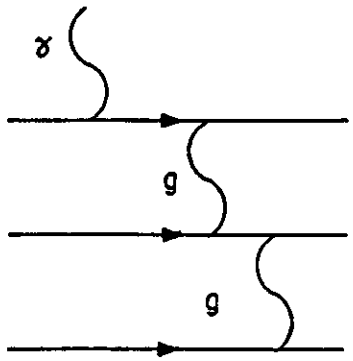

Figure 1. Diagram leading to the prediction (Ca-89) of the Q^2 dependence of $Q^3 A_{1/2}$ of the helicity amplitudes .

At higher Q^2 the existing data consists of inclusive electron scattering cross sections shown in Figure 3. An analysis (Ca-89) of the resonant part in the regions of the first, second and third maxima (see Figure 3) indicate an approach to the predicted Q^2 dependence may occur in the interval $3 < Q^2 < 5\ GeV^2/c^2$. The result of this analysis is shown in the Figure 4. This analysis is limited by the statistical accuracy of the primary inclusive cross sections. Also, the inclusive cross sections consist of the sum of all resonances at a given W, as well as a large underlying non-resonant contributions.

Exclusive angular distribution will be important in providing the possibility of multipole decomposition, and will yield a great deal of reduction of the non-resonant background through the selection of decay channel and decay angle kinematic space.

The magnitudes of the helicity amplitudes are also predicted by pQCD calculations in terms of specific transition density models. The dashed lines in Figure 2 indicate the range of such predictions. Once again, measurements will be required at higher Q^2 than the limits of existing data.

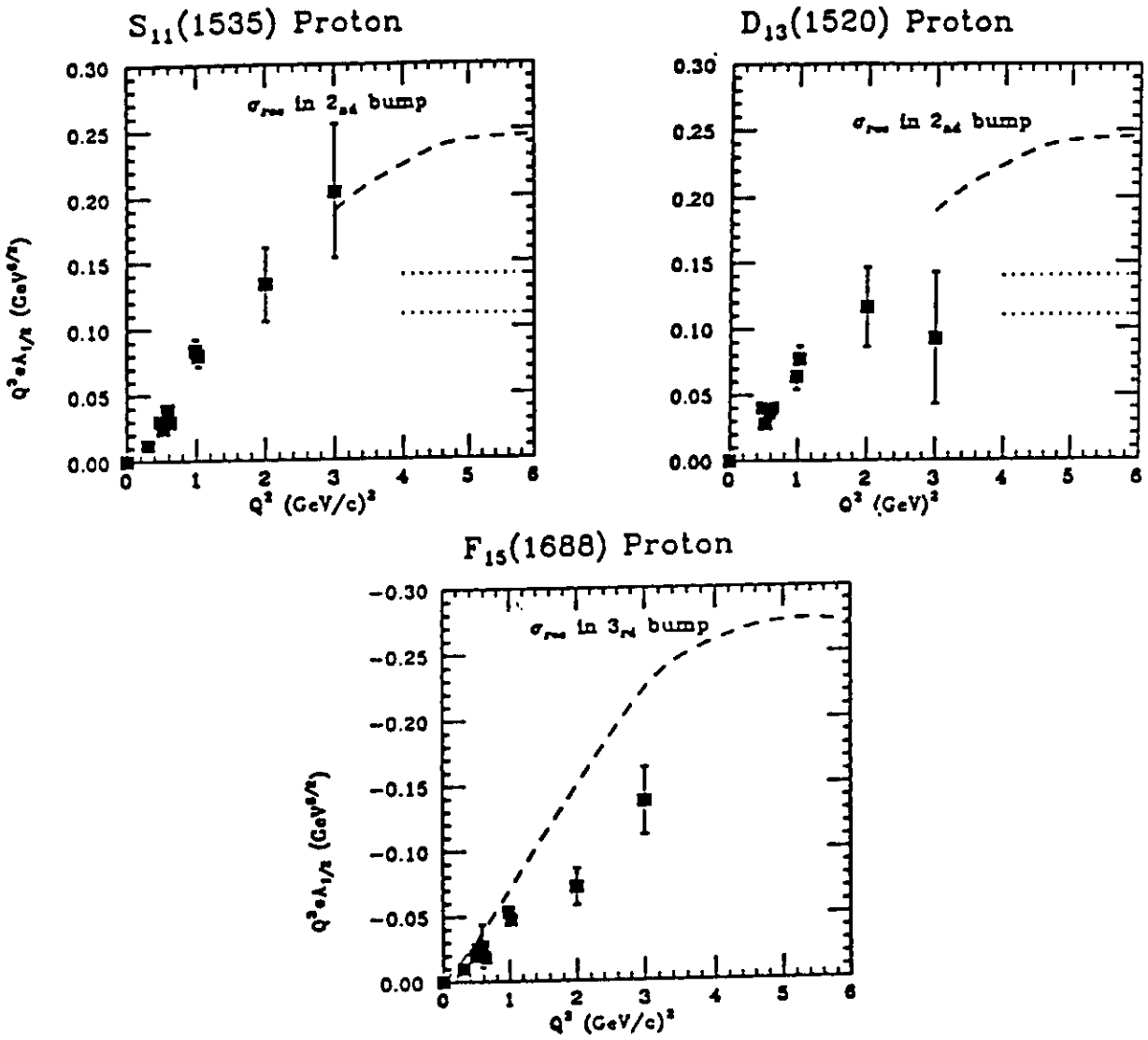

Figure 2. The Q^2 dependence of $Q^3A_{1/2}$ for the $S_{11}(1535)$, $D_{13}(1520)$ and $F_{15}(1688)$ resonances. The dashed curves show the Q^2 dependence of the peaks in the total virtual photon cross section data as in Figure 4, at the respective values of W. The dotted lines are the range of predictions based on QCD sum rules (Ca-89). The figure is from Bu-89.

Other specific examples:

The $S_{11}(1535)$ form factor. This is one of the most interesting transitions to study in that the form factor has an anomalously small Q^2 dependance (see Figure 3) so that it becomes quite dominant for $Q^2 \gtrsim 2$ GeV^2/c^2.

In addition the $S_{11}(1530)$ is one of the few large resonances which has a strong coupling to the η decay channel. At lower Q^2 the reaction $p(e,e'p)\eta$ is totally dominated by s-wave production and exhibits a clear resonant behavior with only small non-resonant contributions (Ba-84). For s-wave production the differential cross section contains only two terms.

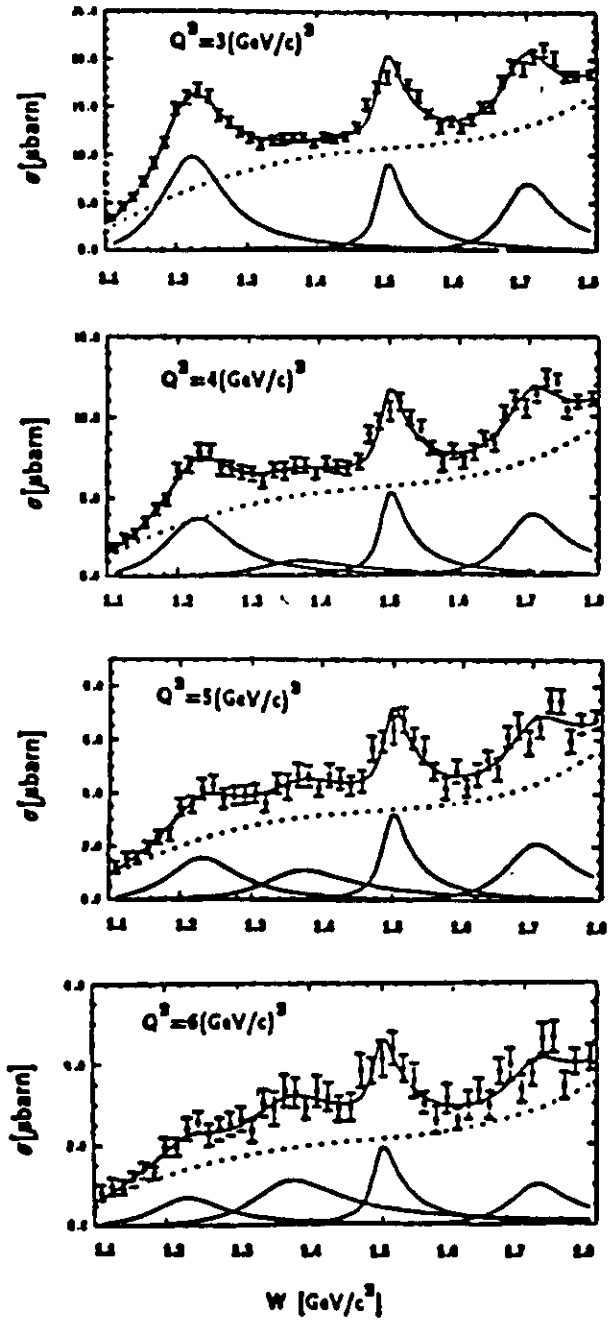

Figure 3. The W dependence of the inclusive electron scattering data for various values of Q^2. The data are from Br-76. The curves are the result of a phenonenalogical analysis, assuming the existence of $P_{33}(1232)$,$P_{11}(1440)$, $S_{11}(1535)$, and $F_{15}(1688)$ resonances indicated by the solid curves, and non-resonant contributions indicated by the dashed curve.

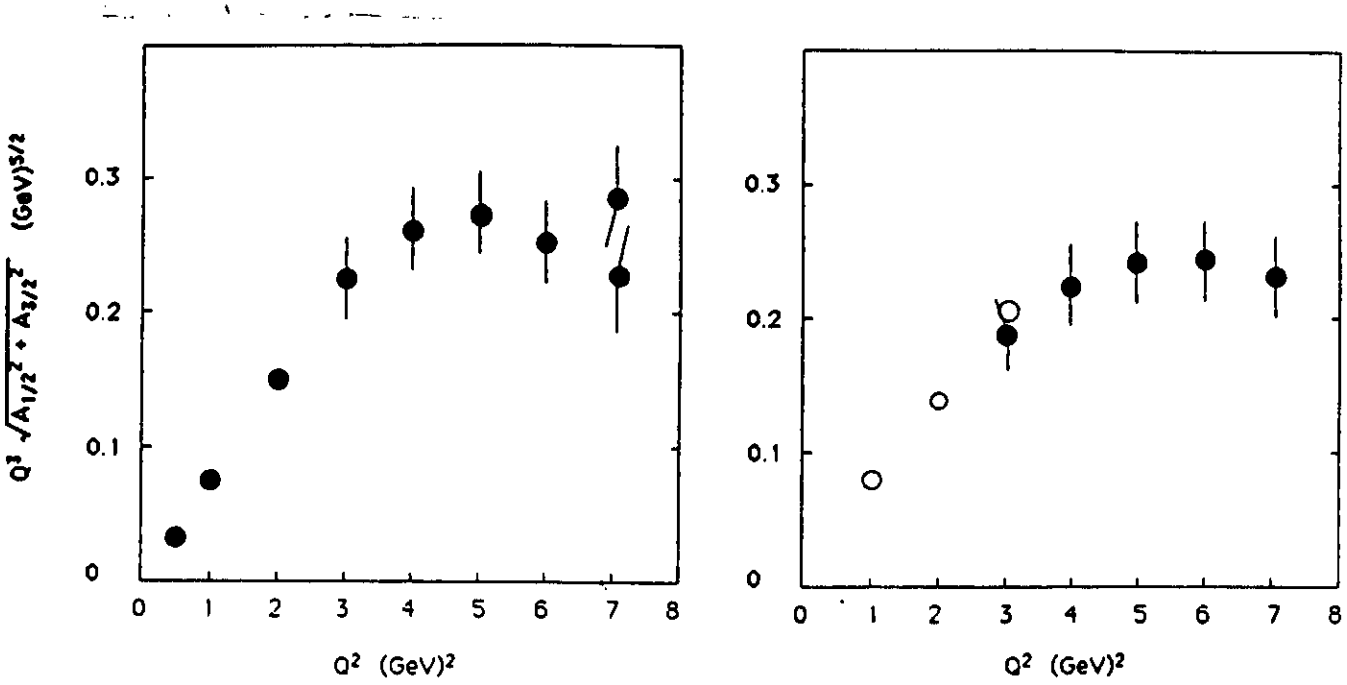

Figure 4. The Q^2 dependence of $Q^3A_{1/2}$ for the peaks in the inclusive cross section (Figure 3) near the centroids of the $S_{11}(1535)$, $D_{13}(1520)$ and $F_{15}(1688)$ resonances.

$$\frac{d\sigma}{d\Omega_\eta} = \frac{|\vec{P}_\eta^*|W}{MK}(|A_{0+}|^2 + \epsilon\frac{Q_0^2}{\bar{Q}^2}|C_{0+}|^2)$$

where

$$K = \frac{W^2 - M^2}{2M}$$

At smaller Q^2, experiments to separate σ_L/σ_T were performed, showing that the longitudinal coupling of the $S_{11}(1535)$ is very small. Therefore the resonant transverse multipoles can be directly extracted from this data, with small corrections due to non-resonant contributions.

These experimentally attractive features will enable us to study this transition at a very early stage in the program.

The $P_{11}(1440)$, or Roper resonance, has been the the subject of considerable interest. In the non-relativistic quark model this state is in an N = 2 oscillator level with the same quantum numbers as the N = 1 nucleon. If it is largely a radial excitation of the nucleon it will be excited primarily by means of longitudinal photons. There has also been speculation that its P_{11} character makes it a candidate for the lightest hybrid baryon. At low Q^2 it is obscured by its proximity to the much more strongly excited delta, which of course is primarily transverse in character. On the other hand, it has been pointed out (Cl-89),that if it is indeed an N = 2 excitation, the Roper resonance may become more strongly excited than states such as the D_{13}. Also, the Δ falls of quite a bit faster than the other strong resonances, leaving the Roper strongly enough excited to possibly be cleanly separated

from the S_{11} and Δ. Support for this idea comes from the available inclusive data (Figure 3) with increasing $Q^2 \sim 5\ GeV^2/c^2$.

It is further noted in Cl-89 that the ratio of $A_{1/2}$ amplitude due to neutron and proton excitation should be -2/3, if the transition were a magnetic excitation of the $(56, 0^+)$. Thus, data on this resonance is needed from a neutron target.

The extraction of longitudinal components of resonances would be extremely difficult with inclusive data. This is because the non-resonant contribution has a large longitudinal component due primarily to the pion-current, or t channel Born diagram which is present exclusively in the π^+ channel. With exclusive experiments, one avoids this by observing non-charged meson production (π^o, or η). Since the t channel is forward peaked in pion angle, even for the π^+ channel, a great deal of background is eliminated by observing the pion emitted at backward angles.

The non-resonant contributions are in themselves physically interesting. Usually they are treated in terms of Born diagrams. At low Q^2 and low t they are dominated by the pionic current term, with s and u channels also contributing significantly. At higher Q^2 and t, the s and u channels are expected to dominate. However, as can be seen in Figure 3, the Q^2 dependence rather appears to track the resonant Q^2 dependence. This phenomenon is known as the Bloom-Gilman duality. Recently, this has been discussed in the framework of QCD (Ca-89a). The explanation seems to grossly account for this behavior, however one really needs a more reliable non-resonant separation to check the theory. It also would make sense to extend this to W > 2 GeV to see how it connects into the scaling region.

A proper treatment of the resonant channels will require a reliable description of the non-resonant channels.

III Experimental Consideration

Event identification: Since the event rate for the proposed experiments will be low, an efficient sorting procedure will have to be implemented. The first level cut will be based on a Cerenkov signal at a rather large angle, indicating the candidacy for an electron involved in a high Q^2 process. Shower counter information should significantly reduce the pion contamination, especially at forward angles. Analysis of drift chamber analog information will also be a powerful tool, especially in the lower momentum regime (p $\sim$ .3 to 1 GeV/c) where the pion dE/dx is near its minimum, while the electron dE/dx has ascended to the fully relativistic value. An assessment of the role of Cerenkov detectors and drift chamber information on the CLAS, relating to experiments of the type proposed here is the subject of a CEBAF-CLAS report (St-89).

The final identification of the event will involve a missing mass reconstruction of the detected particles, thereby identifying the exclusive channel. For a proton target the exclusive single neutral meson channel is clearly isolated by detecting the recoiling proton, and reconstructing the missing mass of the undetected meson. This can be done quite unambiguously, with a moderate resolution ($\sim 10^{-2}$) detection system. Figure 5 shows an example of an experimental missing mass spectrum obtained at DESY (Ba-84) in the study of the reaction $p(e, e'p)\eta$, using spectrometers with a typical resolution of $\delta p/p \sim 1\%$.

This technique is also applicable for $\pi^{+/-}$ production, where the recoiling neutrons and protons are identified by their reconstructed masses.

Simulations of the potential effectiveness of this technique for the CLAS are underway using the codes CELEG (J0-89) and FASTMC (Sm-89). Simulations at lower Q^2 indicate a favorable prognosis for employing this technique with the CLAS. Figure 6 shows a simulated mass spectrum corresponding to a typical kinematic interval in the proposed experiment.

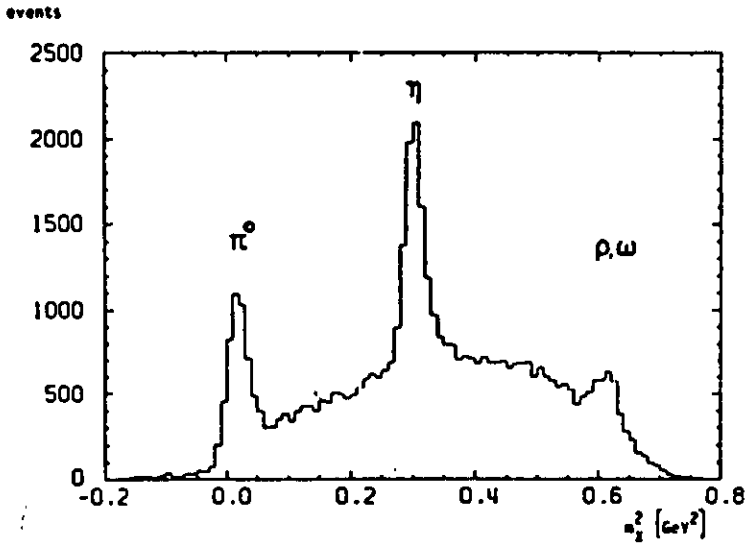

Figure 5. Missing mass spectrum for the reaction $p(e,e'p)X$ clearly showing the η, π^o, and ρ, ω peaks. Data from Br-84

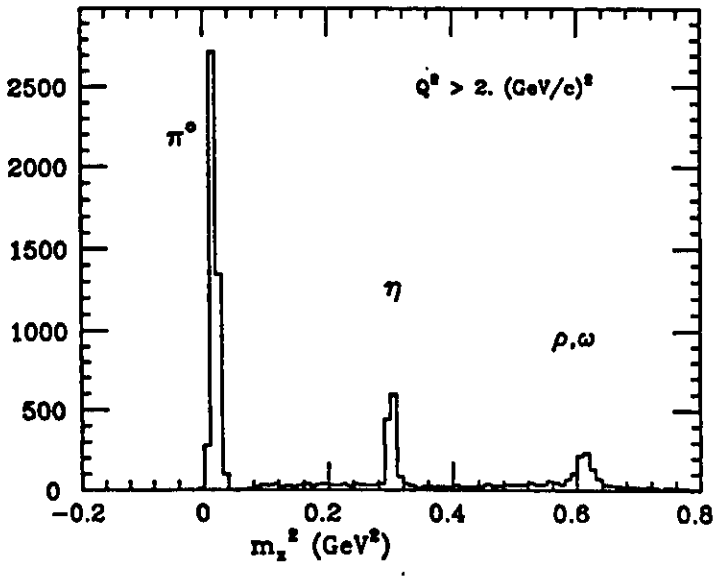

. Figure 6. Simulated missing mass spectrum for the reaction $p(e,e'p)X$ as may be expected for a kinematic setting typical of that for the proposed experiment

Primary experimental limitations are due to a combination of available incident electron energy , and rapidly falling form factors with increasing Q^2, as well as the presence of very important non-resonant contributions at all Q^2.

As with lower Q^2, the goals are to obtain the helicity elements and helicity amplitudes for individual resonances. This decomposition will require angular distribution measurements of the exclusive meson decay channels. An important question is how far one can go with the CLAS, given a given luminosity. Assuming a luminosity of 1×10^{34} we have calculated global rates for exclusive production of various mesons at high Q^2 at the peaks of the $P_{33}(1232)$, $P_{11}(1440)$, $S_{11}(1535)$, and $F_{15}(1688)$, for intervals $\Delta W = 50$ MeV, and $\Delta Q^2 = 1$ GeV^2. The CLAS acceptances were folded in employing the FASTMC.

The estimated resonance global counting rates for a 1000 hr experiment under different experimental conditions are shown in Tables I to III Those for incident electron energy 4 GeV, and initial CLAS detector coverage (full coverage through $\theta_e = 45°$, one sector between $\theta_e = 45°$ through $\theta_e = 90°$) are summarized in Table I. The main limitation in Q^2 is due to the scattered electron angle exceeding the Cerenkov detector coverage. If we require 5000 events as the minimum then we can make significant measurements on the $P_{33}(1232)$, $S_{11}(1535)$, and $F_{15}(1688)$ up to a Q^2 of about 4 GeV^2/c^2. Table II gives the estimates for an incident electron energy of 4 GeV with Cerenkov coverage over all sectors out to an angle of 90°. The net effect is a sixfold increase in events in the range $\theta_e = 45°$ through $\theta_e = 90°$, making possible significant measurements up to $Q^2 = 5$ GeV^2/c^2 on the $P_{33}(1232)$, $P_{11}(1440)$, and $S_{11}(1535)$.

Table III gives the estimates for an incident electron energy of 6 GeV with Cerenkov coverage over all sectors out to an angle of only 45°. Coverage is now significant for all four resonances out to $Q^2 = 5$ GeV^2/c^2, and on the $P_{11}(1440)$, $S_{11}(1535)$, and $F_{15}(1688)$ out to $Q^2 = 6$ GeV^2/c^2. In all cases the electron scattering angle is less than 45°.

References:

(Br-76) F. W. Brasse et al., Nuc. Phys. B110 (1976) 413.
(Br-84) F. W. Brasse et al., Z. Phys. C22 (1984) 33.
Nuc. Phys.B139(1978) 37.
(Br-78) H. Breuker et al., Phys. Lett. 74B (1978) 409.
(Bu-89) V. Burkert, in 'Excited Baryons - 1988', G.
Adams,N.C.Mukhopadhyay,
and P.Stoler,eds.,World Scientific, Singapore (1989), p122.
(Ca-89) C. Carlson, in 'Excited Baryons - 1988', G. Adams
N.C.Mukhopadhyay,
and P.Stoler,eds.,World Scientific, Singapore (1989) p98.
(Ca-89a) C. Carlson and N.C. Mukhopadhyay, Phys. Rev. D, to be
published.
(Cl-89) F. E. Close, Proceedings of the 1988 CEBAF Summer Workshop,
SURA/CEBAF (1989) 75.
(Fo-83) F. Foster and G, Hughes, Rep. Prog. Phys.,46 (1983) 1449
(Jo-89) D. Joyce, CLAS-NOTE 89-004 (1989) unpublished.
(Ha-79) R. Haiden, DESY rep. F71-79/03
(Sm-89) E. Smith, CLAS-NOTE 89-003 (1989) unpublished.
(St-89) P. Stoler, CLAS-NOTE 89-006 (1989) unpublished.

****** $P_{33}(1232)$ ******

Q^2 (GeV^2/c^2)	3	4	5
Rate/1000 hrs =	$.1\times 10^7$	$.2\times 10^6$	$.1\times 10^5$
π^o =	$.2\times 10^6$	$.5\times 10^5$	$.1\times 10^4$
π^+ =	$.8\times 10^5$	$.2\times 10^5$	$.5\times 10^3$

****** $P_{11}(1440)$ ******

Rate/1000 hrs =	*	$.3\times 10^5$	$.1\times 10^5$
π^o =	*	$.8\times 10^3$	$.2\times 10^3$
π^+ =	*	$.1\times 10^4$	$.6\times 10^3$

****** $S_{11}(1535)$ ******

Rate/1000 hrs =	$.3\times 10^7$	$.1\times 10^6$	$.4\times 10^5$
π^o =	$.6\times 10^5$	$.2\times 10^4$	$.6\times 10^3$
π^+ =	$.1\times 10^6$	$.7\times 10^4$	*
η =	$.3\times 10^6$	$.1\times 10^5$	*

****** $F_{15}(1688)$ ******

Rate/1000 hrs =	$.4\times 10^7$	$.1\times 10^6$	*
π^o =	$.7\times 10^5$	$.3\times 10^4$	*
π^+ =	$.2\times 10^6$	$.1\times 10^5$	*

Table I Estimated inclusive rates, and exclusive single meson angle integrated resonance rates, per 1000 hrs. at Q^2 = 3, 4 and 5 GeV^2/c^2. The rates were estimated at the resonance peaks for kinematic intervals dW = 50 MeV, and dQ^2 = 1.0 GeV^2/c^2 The electron beam energy is assumed to be E_1 = 4 GeV, and luminosity = 1×10^{34} $cm^{-2}s^{-1}$. The electron detection coverage is 45° for five sectors, and 90° forone sector of CLAS. Efficiencies were folded in using the code Fast-MC.

****** $P_{33}(1232)$ ******

Q^2 (GeV^2/c^2)	3	4	5
Rate/1000 hrs =	0.1×10^7	0.2×10^6	0.6×10^5
π° =	0.2×10^6	0.5×10^5	$.6\times 10^4$
π^+ =	$.8\times 10^5$	$.2\times 10^5$	$.3\times 10^4$

****** $P_{11}(1440)$ ******

Rate/1000 hrs =	*	$.2\times 10^6$	$.8\times 10^5$
π° =	*	$.5\times 10^4$	$.2\times 10^4$
π^+ =	*	$.7\times 10^4$	$.4\times 10^4$

****** $S_{11}(1535)$ ******

Rate/1000 hrs =	$.3\times 10^7$	$.7\times 10^6$	$.2\times 10^6$
π° =	$.6\times 10^5$	$.1\times 10^5$	$.3\times 10^4$
π^+ =	$.1\times 10^6$	$.4\times 10^5$	$.1\times 10^5$
η =	$.3\times 10^6$	$.6\times 10^5$	$.4\times 10^4$

****** $F_{15}(1688)$ ******

Rate/1000 hrs =	$.4\times 10^7$	$.9\times 10^6$	*
π° =	$.8\times 10^5$	$.2\times 10^5$	*
π^+ =	$.2\times 10^6$	$.6\times 10^5$	*

Table II. As in Table I, but the electron detection coverage is 90° for all six sectors of the CLAS.

****** $P_{33}(1232)$ ******

Q^2 (GeV^2/c^2)	3	4	5	6
Rate/1000 hrs =	$.1\times 10^7$	$.2\times 10^6$	$.7\times 10^5$	$.3\times 10^5$
π^o =	$.2\times 10^6$	$.5\times 10^5$	$.9\times 10^4$	$.3\times 10^4$
π^+ =	$.8\times 10^5$	$.2\times 10^5$	$.3\times 10^4$	$.9\times 10^3$

****** $P_{11}(1440)$ ******

Rate/1000 hrs =	*	$.6\times 10^5$	$.3\times 10^5$	$.2\times 10^5$
π^o =	*	$.7\times 10^4$	$.4\times 10^4$	$.2\times 10^4$
π^+ =	*	$.7\times 10^4$	$.4\times 10^4$	$.2\times 10^4$

****** $S_{11}(1535)$ ******

Rate/1000 hrs =	$.3\times 10^7$	$.8\times 10^6$	$.3\times 10^6$	$.1\times 10^6$
π^o =	$.6\times 10^5$	$.2\times 10^5$	$.6\times 10^4$	$.2\times 10^4$
π^+ =	$.1\times 10^6$	$.4\times 10^5$	$.1\times 10^5$	$.5\times 10^4$
η =	$.3\times 10^6$	$.9\times 10^5$	$.3\times 10^5$	$.1\times 10^5$

****** $F_{15}(1688)$ ******

Rate/1000 hrs =	$.4\times 10^7$	$.1\times 10^7$	$.4\times 10^6$	$.1\times 10^6$
π^o =	$.7\times 10^5$	$.2\times 10^5$	$.6\times 10^5$	$.2\times 10^4$
π^+ =	$.2\times 10^6$	$.5\times 10^5$	$.2\times 10^5$	$.7\times 10^4$

Table III. Table II. As in Table I, but the electron detection coverage is 45° for all six sectors of the CLAS.